

From Gabriele Croci PHD Thesis:

"Development and Characterisation of Micro-Pattern Gaseous Detectors for HEP Applications and Beyond"

University of Siena, December 2010

## Appendix A

# Laboratory Setup

This appendix describes the laboratory setups used for all the measurements reported in the previous chapters.

### A.1 Detectors

#### A.1.1 The Test Detector

The necessity of high flexibility and interchangeability implies the employment of a special designed test detector in order to perform the majority of the measurements. Figure A.1 shows the scheme of such a detector and Figure A.2 shows a photograph of one of these detectors. This basic setup gives the possibility to easily change the number and the type of amplifying structures as well as in the distances between them and the others electrodes (drift and readout). The read-out structure is placed on a fiberglass backplane and it is provided with electrical contacts to allow the acquisition of the signals. The fiberglass plane is used also as support for the high voltage connections. A second fiberglass frame is glued on this plane and includes the gas inlet; the gas outlet is hosted in a third fiberglass frame, that also contains a Kapton or mylar window that allows radiations enter the detector. The frames are assembled using metal screws; a special rubber O-ring, put between the two frames, provides the gas tightness. The detector is always put under the gas flow and two flow meters, one located on the input and the other on the output, monitor the gas tightness.

Inside this support four holes at the four corners are drilled at distances that are needed for the specific measurement. GEMs (shown in Fig. A.3), THGEMs Blind structures, and the drift cathode (usually a full metal-Kapton sheet), are mounted on a square frame that contains

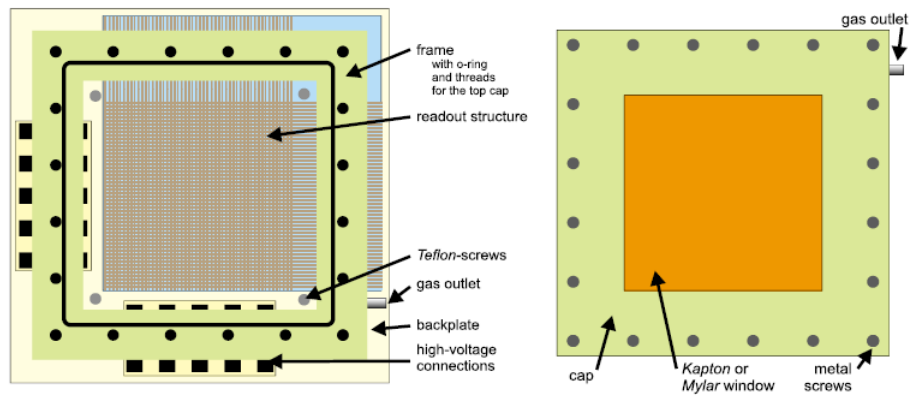


Figure A.1: Schematic view of the special test detector, [43].

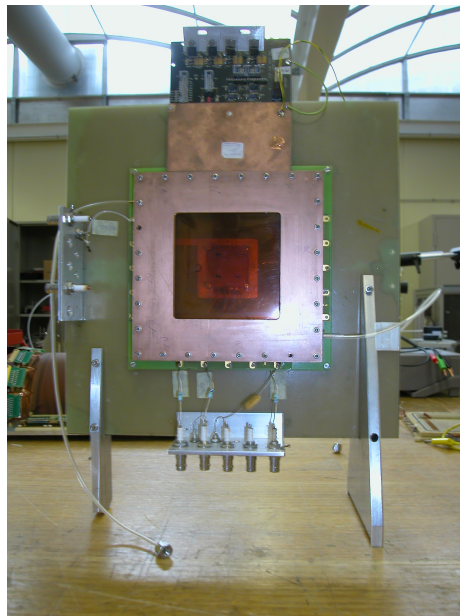


Figure A.2: External view of the test detector.

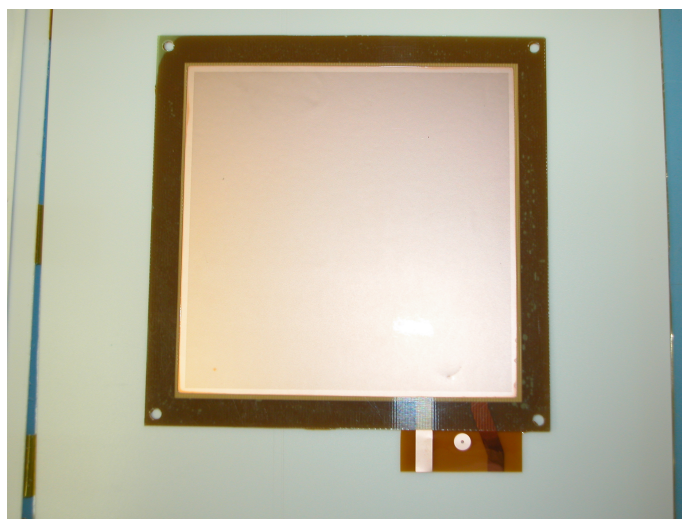


Figure A.3: A standard GEM foil, stretched on its frame.

four holes placed in the corners, inserted in four pillars and kept at the correct distance using insulating spacers of thickness from 0.5 mm to 3.5 mm. These spacers, together with the electrodes frame (usually 0.5 mm or 1 mm thick), define the distances between the different electrodes.

The whole chamber can be mounted on a metal support, fixed to an optical bench rail that allows it to be moved in the three directions and to be rotated.

### A.1.2 The compact glued Triple GEM detector

This kind of detector has been only used for the realization of the Tracking Triple GEMs chambers used in the commissioning of the RD51 telescope. In this case, once the detector is built, it can not be modified since all the frames are glued together. A detailed description of this type of Triple-GEMs is given in Chapter 8. The high voltage is delivered using the resistor divider described in Fig. A.4.

## A.2 Laboratory Facilities

### A.2.1 Radiation Sources

The main source used in our experiments is a collimated beam of soft X-Rays. The X-rays tube has a Cu-Target and, as a consequence, the produced X-Rays have an energy of 8.9 KeV. X-rays are produced by electrons, that are accelerated by a potential difference

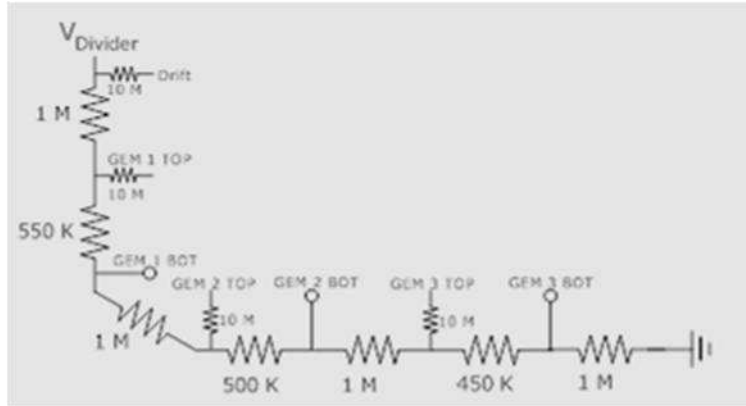


Figure A.4: Resistor divider used for glued detectors.

of at least 10 kV, hitting the copper target. These electrons are generated by thermoionic emission from a metal filament. The number of emitted electrons (the electron current) can be changed by manually increasing or decreasing the temperature of the filament. The rate of the X-rays beam is directly dependent on this current: an higher electron current results in a larger number of electrons interacting with the copper target and, as a consequence, in a higher number of produced photons. The intensity of the beam can be chosen by changing the filament current in a range from 0.04 mA to 4 mA. Even if the filament current has the lowest value, the flux will be rather high. To further reduce the rate, additional copper absorbers can be directly mounted on the exit of the collimator. A remotely activated shutter, placed in front of the beam, allows to stop the irradiation.

The profile of the emitted beam is a Gaussian one and X-rays are sent to the detector using different opening collimators. The generator is mounted on an optical bench, allowing movement towards different directions.

In addition to the already describer Cu X-Rays tube, also a  $^{55}\text{Fe}$  source (yielding X-Rays of 5.9 KeV) and a  $^{90}\text{Sr}$  beta-emitter (2 MBq activity) can be used in some specific measurements.

### A.2.2 High Voltage power supply

The high voltage can be supplied to the detector in two different ways: using a voltage divider or through separate power supplies. The voltage divider (see Fig. A.4) is safer for the integrity of GEMs, because in case of a discharge, there is a global decrease of the voltage,

avoiding the possibility of getting too high electric fields in the detector. Using the values of resistor described in Fig. A.4), a current of about  $700 \mu\text{A}$  has to flow in the circuit in order to get sufficiently high potential differences on the GEMs ( $\Delta V_{GEM} > 300 \text{ V}$ ). Since such a high current must be used to supply high voltage to the GEM, these resistors' values guarantee that the gain of GEMs will not change also if a very high particle rate interacts with the chamber and, as a consequence, a very high ionization current (few nA) is present in the gas volume. This kind of power supply delivery was chosen for the realization of RD51 Tracking telescope GEMs. The power supply unit used in this case is the CAEN N470 that is able to deliver a maximum voltage of 8 kV and a maximum current of 1 mA.

The use of separate power supplies can result in irreversible damages to the detector, but sometimes it is necessary because it allows to easily modify the operating voltages of the detector. Using this technique, it is mandatory to install a  $1 \text{ M}\Omega$  resistor between the HV contact and the electrodes contact; in case of discharges, this resistor reduces the applied potential faster than the current limit does in the power supply. In this case, several CAEN N471A HV power supplies units (Max V = 8 kV, Max I =  $8 \mu\text{A}$ ) are used.

### A.2.3 Gas System

The gas mixture employed in all the measurements was a mixture of a noble gas and a quencher. The choice was always a mixture of Argon (Ar) and Carbon-Dioxide ( $\text{CO}_2$ ) in different percentages. Mixtures like this are relatively cheap, non-toxic and non-flammable. The measurements were performed either using a complete gas mixing system in which it is possible to vary the relative amount of the two gases, or employing premixed bottles. The gas flow is always around 5 l/h that corresponds to an exchange of 5 detector's volumes during 1 hour.

## A.3 Standard Measurements Description

### A.3.1 Pulse Height Measurements and Energy Resolution determination

Detector characterization usually starts with the acquisition of a pulse height spectrum (PH) for fixed detector electrostatic field configuration. This measurement is performed by using a full metal readout pad as an anode; if the detector is provided with a padded or with a strips readout, all the pads/strips will be connected together. The electronic signal induced on the

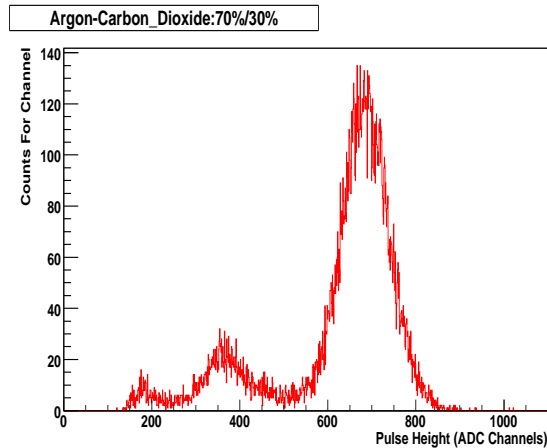


Figure A.5: Single GEM Pulse Height Spectrum acquired with Fe source, the lowest peak on the right is noise.

anode by the movement of the avalanche electrons in the induction gap is preamplified by a preamplifier (ORTEC preamplifier 142IH, see later for a complete description) and then sent to a shaping amplifier (ORTEC 450 Research Amplifier, see later for details). The signal is then split and processed by a NIM electronics architecture: a part of it is discriminated in order to create the logic gate signal for the Analog to Digital Converter (CAMAC ADC, Lecroy 2249W) and the other is directly sent to the ADC. The output of the ADC is then sent to a computer connected to the CAMAC Controller where data are processed and stored. The output data for a detector operated with Argon-based gas mixtures is the one shown in Fig. A.5

This spectrum was acquired using an X-Rays Iron source whose main emission line is located at 5.9 KeV. The histogram shows that this line (the peak located at 700 ADC channels) is visible and that another small peak is present at half range (350 ADC Channels) with respect to the main one (the electronic pedestal is located at the zero ADC channel). In addition to the absorption of the whole photon energy, there is a competitive process in Argon-based gas mixtures. If the energy of X-Rays is greater than the threshold for the argon K-shell ionization (3.203 keV), the photon might extract a photoelectron from an inner Argon shell, as the K-shell. This K-shell vacancy is then filled by an electron coming from an outer shell and, consequentially, a de-excitation X-Ray, whose energy corresponds to the energy difference between the levels (usually 2.9 keV), is emitted from the atom. If this photon escapes from the detector, an amount of energy equal to the energy of the escaped

photon is lost. Since this energy has a lower energy, it will have a very high probability to be re-absorbed in the gas. Nevertheless, there is a non negligible probability (15%) that this de-excitation photon escapes from the detector; in this case, the amount of photon energy is lost. Initial X-rays will still create ion/electron pairs (through photoelectric absorption) but the number of such pairs will be lower. In this case, a signal can still be collected, but its size is lower than the one of the incident photon by an amount equal that is to the energy of the photon. Therefore, the typical PH spectrum shows two peaks: the first one is placed at the total energy deposited by the X-Rays and the second one, the Argon escape peak, is placed at an energy that is 3.2 keV lower than the energy of the interaction photon (3 keV for Fe).

The energy resolution is defined as  $\frac{FWHM}{PeakPosition}$  and is measured by fitting the main peak. For a GEM-based detector, its standard value is around 20% (FWHM) at 5.9 keV.

Measurements that are performed through the above described method are referred in the text as measurements in *PH mode*.

### A.3.2 Effective Gain Measurements

These measurements are always performed by employing the Copper X-Rays beam coming from the X-Rays generator, since high photon rates are required.

The effective gain is measured for different interaction rates as:

$$G_{eff} = \frac{I_{ReadOut}}{n_{tot} \cdot F \cdot e} \quad (A.1)$$

where  $I$  is the electronic current in Ampere measured on the readout anode,  $F$  is the interaction flux,  $e$  represents the electron unit charge and  $n_{tot}$  is the number of primary ionization pairs. At very high fluxes, the pile up effect can lead to an imprecise measurement of the interaction flux itself. In order to avoid this problem, it is necessary to reduce the rate by putting a copper attenuator out of the collimator of the X-Rays generator. Knowing the attenuation factor, it is possible to correctly estimate the real rate and to consequentially define the gain.

The photon interaction rate is determined by counting the number of pulses for the highest safe voltage; the number of pulses that are recorded by a CAEN Scaler N145 in a certain time period gives the information about the rate

The determination of the gas avalanche effective gain dependence on the potential difference of the amplification region is performed through an amplification voltage scanning. This

voltage difference is increased from low values (for example 100 V for a Standard GEM in Ar/CO<sub>2</sub> 70%/30%) up to the maximum possible value before the appearing of spontaneous discharges (520 V for a Standard GEM in Ar/CO<sub>2</sub> 70%/30%) and the electronic current on the anode and is measured using a very precise picoamperometer (Keithley 6517A, see below for more details). The anodic electronic current will be higher if a higher potential difference is applied since the gas gain increases.

The result of an effective gain measurement of three Triple-GEM detectors is shown in Fig. 8.6.

The space uniformity of the gain can be obtained by measuring the gain in different spots of the detector active area.

Measurements that are performed through the above described method are referred in the text as measurements in *Current mode*.

### A.3.3 Scans of External Fields

The influence of the external fields (Drift, Transfer and Induction fields) is determined by changing their values one by one and keeping fixed all the other parameters; for each value a PH or a current measurement is performed.

### A.3.4 Measurements of Rate Capability

The goal of this measurement is to understand if the detector gain shows a loss, due to the space charge effect, starting from a specific value of the photon interaction rate. It is performed using the Copper X-Rays generator since it is possible to get interaction rates up to  $10^6$  Hz/mm<sup>2</sup>. This measurement is divided into two steps: firstly the interaction rate is determined for different Copper X-Rays generator currents by making a PH mode measurement; after the electronic current on the anode is measured for each point. Finally, the gain is evaluated using formula A.1. Two examples of rate capability measurements are shown in Fig. 8.8 for a Triple GEM detector and in Fig. 7.30 for a Resistive Blind GEM.

### A.3.5 Time Stability Measurements

These measurements are performed in order to understand if the effective gain shows any variation with time. The most important ones are shortly summarized in the following:



1. *Same Time Measurements*: apply high voltage to all the electrodes, immediately start to irradiate the chamber and acquire successive PH spectra
2. *Very Low Rate Measurements*: they are similar to SAME TIME but, in this case the chamber is only irradiated every 5 minutes for the minimum time needed to acquire a pulse height spectrum. The interaction rate is around few hertz.
3. *On Before Measurements*: apply high voltage to the chamber some hours before starting irradiation; acquire successive PH spectra.
4. *Position Scans*: acquire a spectrum in a long time ( $\geq 5$  hours) irradiated point; move the x-ray source and acquire spectra in neighbouring points.

The gain variation is evaluated by fitting all the acquired spectra.

### A.3.6 Discharge Probability Measurements

The occurrence of discharges inside micro pattern detectors is one of the biggest operating problems. Since non uniform and intense field are present in MPGDs especially at sharp edges and at the boundaries between metallic and dielectric material, there is the possibility that discharges develop inside these detectors. These phenomena can be a disastrous for the detector since they can ruin the detector itself and the read-out electronics. It is fundamental to avoid these discharges as much as possible but, since it is not possible to completely exclude them, the detector itself has to be able to support a small rate of breakdowns.

The measurement of the discharge probability of a detector is performed by introducing highly ionizing particles in the gas flow. As illustrated in Fig. A.6, a thorium  $^{198}\text{Th}$  source is inserted in the gas flow. The thorium decays to Radon, that, being a gas, is driven inside the detector. Radon emits high energetic alpha particles (5 MeV), that are able to trigger a discharge.

The measurement is subdivided into two steps: first of all, a very low amplification voltage is set and the alpha particle rate is measured in PH mode: this permits to understand how many alpha particles are present in the gas volume per time unit. Once the rate is determined, the amplification voltage is increased and the current on the electrode is readout: if this current exceeds some predefined thresholds (usually around  $1\ \mu\text{A}$ ), the discharge counter will be incremented. The discharge probability for each operating voltage is defined as the ratio

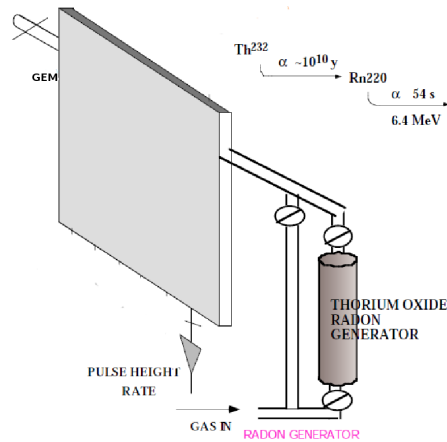


Figure A.6: Discharge Probability Measurements Experimental Setup.

between the number of observed discharges in a certain period of time and the alpha particle rate. An example of such a measurement is shown in Fig. 8.11.

## A.4 Laboratory Instruments

### A.4.1 Ortec 142 IH Preamplifier

The ORTEC Model 142IH is a Charge-Sensitive Preamplifier. It accommodates any detector capacitance up to 2000 pF. The preamplifier includes a built-in protection network to prevent damage to the input FET from inadvertently applied over-voltages or from sparks coming from the detector.

Its noise increases with higher input capacitance. From 0 to 100 pF it is 27 eV/pF and from 100 pF to 1000 pF it is 34 eV/pF. Its rise time from 10% to 90% of peak amplitude is less than 20 ns at 0 pF and lower than 50 ns at 100 pF. The preamplifier energy range is 0 to 100 MeV-Si, its dynamic input capacitance is 10,000 pF and its integral nonlinearity is lower than 0.05%

The preamplifier accepts input signal from the detector; there is also the possibility to input a test pulse in order to verify the calibration of the DAQ system. Depending on the kind of measurement that has to be performed, it has both time and energy outputs.

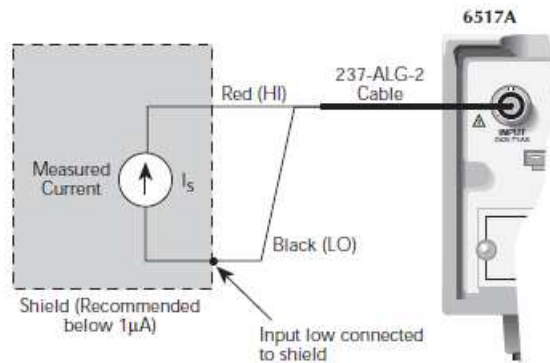


Figure A.7: Method for current measurements using the Keithley 6517A model.

#### A.4.2 Ortec 450 Research Amplifier

This module receives the pulse from the preamplifier and it is able to amplify, filter and shape it. It is able to produce bipolar, fast bipolar and unipolar output. The unipolar output (the one that is always used in the measurements) has a selectable pulse shape for optimum filtering and baseline restoration for low-frequency noise reduction. The frequency bandpass through this output ranges from 100 Hz to 15 MHz and the gain ranges from 4 to 5000. The module produces semi-Gaussian shaped pulses by employing an active-filter network whose differentiation and integration shaping times are selected by the user. Both integrate low-pass filter and differentiate high-pass filter shaping time can be set at 0.1, 0.2, 0.5, 1, 1.5, 2, 3, 5, 10  $\mu$ s. The output impedance of this amplifier is lower than 0.1  $\Omega$  and it has the possibility to eliminate the pulse undershoot, thanks to a pole-zero cancellation network whose parameters are defined by the user.

#### A.4.3 Keithley 6517A High Resistivity Meter

This instrument has a very high internal resistor (up to T $\Omega$ ) and, consequentially, is gives the possibility to measure very low currents up to few pA with a resolution of 1 pA. The instrument is connected to the device under test (DUT) through a tri-axial cable. The measurement of the current is performed by acquiring a user-defined number of samples during one second, by subtracting an offset value that can be set by the user, and by averaging the five subtracted values. The Keithley is remotely controlled through a GPIB-USB interface by a computer where a Labview program is installed that sends commands to the instrument.

#### A.4.4 Data Acquisition System

The signal coming from the detector is preamplified using an ORTEC or a CAEN preamplifier and then it is amplified using a research amplifier. Then the signal is processed using NIM modular electronics and it is recorded using a CAMAC system (CAMAC Controller 116A and LeCroy Charge ADCs 2249A and 2249W). The CAMAC controller is connected to a computer where data were stored.